Gondwana Research xxx (2013) xxx–xxx

Contents lists available at SciVerse ScienceDirect

Gondwana Research

journal homepage: www.elsevier.com/locate/gr

Provenance of Late Triassic sediments in central Lhasa terrane, Tibet and its implication

Guangwei Li [a,b,*], Mike Sandiford [b], Xiaohan Liu [c], Zhiqin Xu [a], Lijie Wei [c], Huaqi Li [a]

[a] State Laboratory for Continental tectonics and Dynamics, Institute of Geology, Chinese Academy of Geological Sciences, Beijing 100037, China
[b] School of Earth Sciences, University of Melbourne, Victoria 3010, Australia
[c] Key Laboratory of Continental Collision and Plateau Uplift, Institute of Tibetan Plateau Research, Chinese Academy of Sciences, Beijing 100085, China

ARTICLE INFO

Article history:
Received 16 January 2013
Received in revised form 14 June 2013
Accepted 15 June 2013
Available online xxxx

Handling Editor: G.C. Zhao

Keywords:
Provenance
Late Triassic
Lhasa terrane
Chronology
Hf isotopes

ABSTRACT

In southern Tibet, Late Triassic sequences are especially important to understanding the assembly of the Lhasa terrane prior to Indo-Asian collision. We report new data relevant to the provenance of a Late Triassic clastic sequence from the Mailonggang Formation in the central Lhasa terrane, Tibet. Petrographic studies and detrital heavy mineral assemblages indicate a proximal orogenic provenance, including volcanic, sedimentary and some ultramafic and metamorphic rocks. In situ detrital zircon Hf and U–Pb isotope data are consistent with derivation of these rocks from nearby Triassic magmatic rocks and basement that comprise part of the newly recognized Late Permian–Triassic Sumdo–Cuoqen orogenic belt. The new data suggests correlation with the Upper Triassic Langjiexue Group which lies on the opposing (southern) side of Indus–Yarlung ophiolite. Sediments from both the Mailonggang Formation and Langjiexue Group are interpreted to represent formerly contiguous parts of a sequence deposited on the southern flanks of the Sumdo–Cuoqen belt.

1. Introduction

The geology of Tibetan Plateau has received considerable geologic attention with much of this work being focused on the processes attendant to the ongoing collision of India and Asia (e.g. Molnar and Tapponnier, 1975; England and Searle, 1986; Tapponnier et al., 2001; Ding et al., 2005; Aitchison et al., 2007). In contrast, the pre-collisional and early collisional history of southern Tibet is relatively poorly understood. However, some recent important discoveries have begun to shed new light on this hitherto enigmatic phase. Firstly, the discovery of the Paleozoic eclogite, igneous rocks and metamorphic events at Sumdo to the northeast of Lhasa city suggest the existence of a previously unrecognized Permo-Triassic orogenic zone within the central Lhasa terrane, termed the Sumdo–Cuoqen belt (Chen et al., 2009; Yang et al., 2009; Zhu et al., 2009; C.Y. Dong et al., 2011; Li et al., 2011; X. Dong et al., 2011). Secondly, our recent investigations have suggested that the boundary between India and Asia may extend to the south of the Indus–Yarlung suture zone (IYSZ, Liu et al., 2010, 2012). In addition, new paleomagnetic data have been used to suggest a more complex, multi-phase collisional history than have been traditionally envisaged (Aitchison et al., 2007; Cai et al., 2012; van Hinsbergen et al., 2012). Finally, Zhu et al. (2011, 2013) have proposed that the Lhasa terrane derives from a continental fragment rifted from the Australian Gondwanan margin.

These discoveries and interpretations call into question some traditional view concerning the pre-and early collisional history of southern Tibet, and raise a raft of new questions. The Paleozoic–Mesozoic sedimentary sequences in Lhasa terrane provide a key to clarify these questions. In this study, we focus on the Late Triassic sedimentary sequences in the central Lhasa terrane. We use petrographic and detrital zircon isotopic data to constrain the provenance of the sediments. We also compare our data with that from the Late Triassic sequences on the south side of the Indus–Yarlung Zangbo ophiolite and in combination with the magmatic, tectonic and metamorphic constraints, and explore the implications of these Late Triassic sequences for the evolution of Lhasa terrane.

2. Geological setting of Lhasa terrane

Tibet is underlain by four E–W trending geologic terranes. From north to south, these are the Songpan–Ganzi, Qiangtang, Lhasa and the Himalaya terranes. Each is separated from the other by inferred sutures that from north to south are (1) Jinshajiang suture (JSS), (2) Bangong–Nujiang suture (BNS), and (3) Indus–Yarlung suture (IYS). These represent the multi-phase Tethyan Ocean relics, respectively (Yin and Harrison, 2000; Yin, 2006; Fig. 1).

* Corresponding author at: School of Earth Sciences, University of Melbourne, McCoy Building, Corner Swanston & Elgin streets, Parkville, Victoria 3010, Australia. Tel.: +61 3 90357571; fax: +61 3 83447761.
E-mail address: guangwei.li@unimelb.edu.au (G. Li).

1342-937X/$ – see front matter.
http://dx.doi.org/10.1016/j.gr.2013.06.019

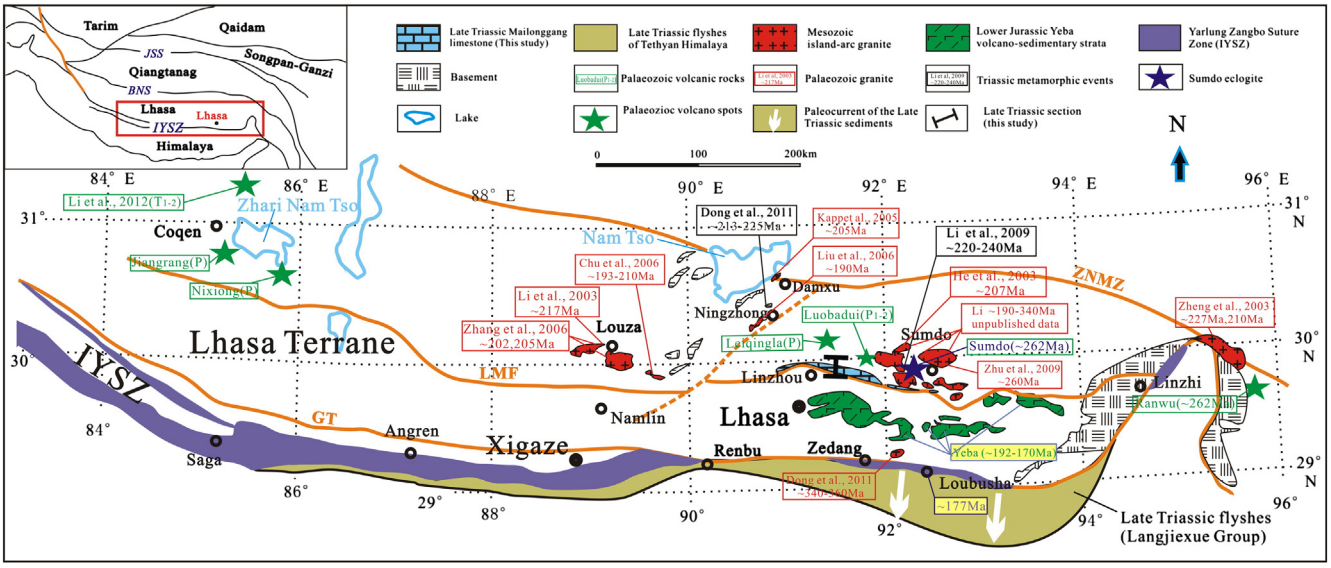

Fig. 1. The distributions of the basement rocks, Paleozic–Early Mesozoic magmatic rocks in Lhasa block, south Tibet. LMF, Luobadui–Milashan Fault; ZNMZ, Shiquan River–Nam Tsomelange zone.
Modified from Zhu et al. (2008), X. Dong et al. (2011), Zhu et al. (2013).

The Lhasa terrane extends more than 2000 km east to west and 200–300 km north–south. In the west it is truncated by the Karakoram strike-slip fault, and in the east it bends southward around the eastern Himalaya syntaxis (Dewey et al., 1988; Yin, 2006). It can be subdivided into the southern, central and northern Lhasa terranes, which are separated by the Shiquan River–Nam Tso mélange zone (SNMZ) to the north and Luobadui–Milashan Fault (LMF) to the south, respectively (Zhu et al., 2013, Fig. 1). The southern Lhasa terrane is characterized predominantly by Mesozoic–Cenozoic intrusive and volcanic rocks of the Gangdese arc. This includes the Early Jurassic Yeba and Tertiary Linzicong volcano–sedimentary rocks (Chu et al., 2006; Mo et al., 2007; Zhu et al., 2008; Ji et al., 2009; Zhu et al., 2010, 2013), as well as minor Mesozoic–Cenozoic sedimentary strata (Leier et al., 2007). Meanwhile, Precambrian crystalline basements occur locally in the Linzhi and Chayu areas (C.Y. Dong et al., 2011; X. Dong et al., 2011; Zhu et al., 2013). The northern Lhasa terrane comprises mainly Late Jurassic–Early Cretaceous sedimentary sequences (Yin et al., 1988; Leier et al., 2007), with some Mesozoic (mainly Cretaceous) volcano–sedimentary rocks and plutonic rocks (Zhu et al., 2011, 2013). The northern Lhasa thrust belt was tectonically active from the Cretaceous through to the Eocene (Kapp et al., 2007), prior to and during the early stages of India–Asia collision.

In the central Lhasa terrane, it exposes the Proterozoic to Early Cambrian metamorphic basement in the Nyainqentanglha area, and is covered with widespread Permo-Carboniferous metasedimentary rocks and small amounts of well-exposed Ordovician, Silurian, and Devonian strata, and Triassic limestone as well (Pan et al., 2006; Zhu et al., 2013). Paleozoic coesite-bearing eclogites have been documented in an E–W trending belt at least hundred km long the central Lhasa terrane, also named the Sumdo–Cuoqen belt (Chen et al., 2009; Li et al., 2009; Yang et al., 2009; Li et al., 2011; Fig. 1). The P-T for these eclogite conditions is estimated to be higher than 2.7 GPa and 730 °C, with coesite pseudomorphs implying high to ultra-high pressure conditions (Chen et al., 2009; L.S. Zeng et al., 2009; Q.G. Zeng et al., 2009; Yang et al., 2009). The geochemistry and Sr–Nd isotope analysis suggest a typical MORB affinity for the protolith rocks of the eclogites (Chen et al., 2009). Eclogites in fault contact with the garnet-bearing, muscovite–quartz schist in the Sumdo region have U–Pb zircon ages of 262 ± 5 Ma (Chen et al., 2008), while metamorphic zircon ages of ~225–212 Ma are reported from the Nyainqentagnlha area (X. Dong et al., 2011). Muscovite and amphibole from the adjacent muscovite–quartz schists and from the eclogites have Mid–Late Triassic ^{40}Ar–^{39}Ar ages in the range of 220–240 Ma (Li et al., 2009, 2011). Magmatism associated with this orogenic event include: (1) the Early and Middle Permian volcanic rocks that are exposed locally from Coqen in the west to Ranwu in the east (Geng et al., 2007; Zhu et al., 2010; Fig. 1); (2) the Late-Permian peraluminous granite at Pikang (Zhu et al., 2009); and (3) the Early–Middle Triassic volcanics (Li et al., 2012), and Late Triassic granites found in several areas (Li et al., 2003; Zheng et al., 2003; Kapp et al., 2005; Chu et al., 2006; He et al., 2006; K. Liu et al., 2006; Q.X. Liu et al., 2006; Zhang et al., 2007; Zhu et al., 2011, 2013). The latter may be attributed to the extension after the Late Permian–Triassic compression (Zhu et al., 2013) or the rifting of Lhasa terrane from Gondwana (Fig. 1).

3. Stratigraphy

Our study region is located in the central portion of the Lhasa terrane, in the Damxung-Linzhou area (Fig. 1), in a zone comprising mostly Ordovician to Tertiary strata. The Paleozoic sedimentary strata consist primarily of Carboniferous sandstone, metasandstone, shale and phyllite, with subordinate Ordovician, Silurian and Permian limestone together with interbedded mafic and felsic volcanic rocks. Triassic rocks are defined mainly by the Late Triassic Mailonggang Formation, with rare exposures of Early Triassic strata of the Chaqupu Formation. The Mailonggang Formation includes a large suite of limestone interbedded with sandstone and mudstone, which occur in thrusts contact above Cenozoic clastic sandstone of the K_2 Shexing Formation. The Early Jurassic Jialapu Group is composed of conglomerates, mudstone, and partly volcanoclastic sandstones, locally intruded by the Cenozoic granites. The Upper Jurassic Duodigou Group is made up of littoral facies carbonate. Cretaceous and Tertiary strata consist of clastic mudstone, sandstone and local conglomerate units and arkosic fluvial sandstone and mudstone successions (Li, 1990; Leier et al., 2007; Pullen et al., 2008). In central Lhasa, a northward -propagating retroarc thrust belt (Lhasa–Damxung thrust) developed between the Luobadui–Milashan fault and the Shiquan River–Nam Tso mélange zone (Fig. 1) has emplaced Paleozoic and Mesozoic strata over Cenozoic sequences, and was active between 105 and 53 Ma (Kapp et al., 2007). Tertiary Linzizong volcanic rocks unconformably over the Late Cretaceous clastic rocks (Mo et al., 2007).

In the study region, the Upper Triassic Mailonggang Formation consists of thick-bedded micritic limestones, interbedded with shale and siltstone in the upper parts of the succession, and clastic/lithic sandstone

Please cite this article as: Li, G., et al., Provenance of Late Triassic sediments in central Lhasa terrane, Tibet and its implication, Gondwana Research (2013), http://dx.doi.org/10.1016/j.gr.2013.06.019

in the lower section (Fig. 2). Corals (*Distichophyllia*, *Margarosmilia*, *Margarophyllia*), bivalves (*Trigonia* cf. *Jingguensis*, *Lilangina nobilis*, *Indopecten*, *Pergomidia*) (Fig. 2F), conodonts and occasionally ammonite fragments (*Nevadites*) indicate a time range from Carnian to Norian (Ji et al., 2003). Abundant mud cracks indicate near-shore partly tidal depositonal environments, while chert debris flows within the limestones and common load structures (see Fig. 2 A, B, C) may be attributed to earthquake related-shaking during deposition. In sum, the assemblage of fossils, lithology and sedimentary structures imply a tectonically active, shallow water mixed carbonate–clastic platform environments.

4. Petrography of Mailonggang Formation sandstones

We sampled seven sandstones (LZ11-2-5-1, LZ11-2-5-2, LZ11-2-6, LZ11-2-7, LZ11-2-8, LZ11-2-9, LZ11-2-11) and several limestone samples from the Mailonggang Formation for petrographic observation, heavy mineral statistics and detrital zircon analysis (see Appendix A). The stratigraphic positions of the sandstone samples are illustrated in Fig. 2 (see Appendix A).

Mailonggang Formation sandstones are typically poorly sorted with mostly angular to subangular shapes, implying low maturity consistent with relatively proximal provenances. Quartz (71–74%) includes both monocrystalline and polycrystalline (chert) grains with Qm/Qt value ranging of 59.6% ~ 75%. Feldspar constitutes 3–11% of the rock and is commonly twinned. Lithic clasts (16–24%) are commonly defined by volcanic fragments, sedimentary clasts, metamorphic lithics, and occasionally serpentinized ultramafic fragments reported by Li (1990). For individual samples a total of 300–400 points were counted using the Gazzi–Dickinson method (Dickinson and Suczek, 1979) and plotted on ternary diagrams. The samples studied in this work plot within the collisional orogen field on a Qp-Lv-Ls diagram and within the recycled orogen provenance field on Qt-F-L and Qm-F-Lt diagrams (Fig. 3).

Detrital heavy mineral suites are composed primarily of zircon, apatite, tourmaline, rutile, anatase, leucoxene, magnetite, limonite, and sporadic biotite, chromite, amphibole and barite and epidote. Using the heavy mineral assemblages analysis proposed by Morton and Hallsworth (1994), we calculated the index values (ATi, RZi, and CZi, respectively) (see Appendix A). A wide variation of the ATi values in these samples, range from 2 to 100 with especially low values in the samples from the middle part of section, indicate that some samples were probably derived from the recycled sediments (but it can't be completely excluded the greater apatite loss makes the ATi values lower during transport, deposition and diagenesis); and some with high ATi values indicate that igneous rocks were major contributors. The RZi values are relatively low (mostly around 5) in the sequence. CZi values are generally very low in the section, with the exception of one sample (Lz11-2-8) which indicates a locally significant contribution from ultramafic rocks. Generally, the heavy mineral assemblages of sandstones are consistent with a mixed provenance includes volcanic, magmatic, sedimentary and ultramafic rocks, and maybe some metamorphic rocks.

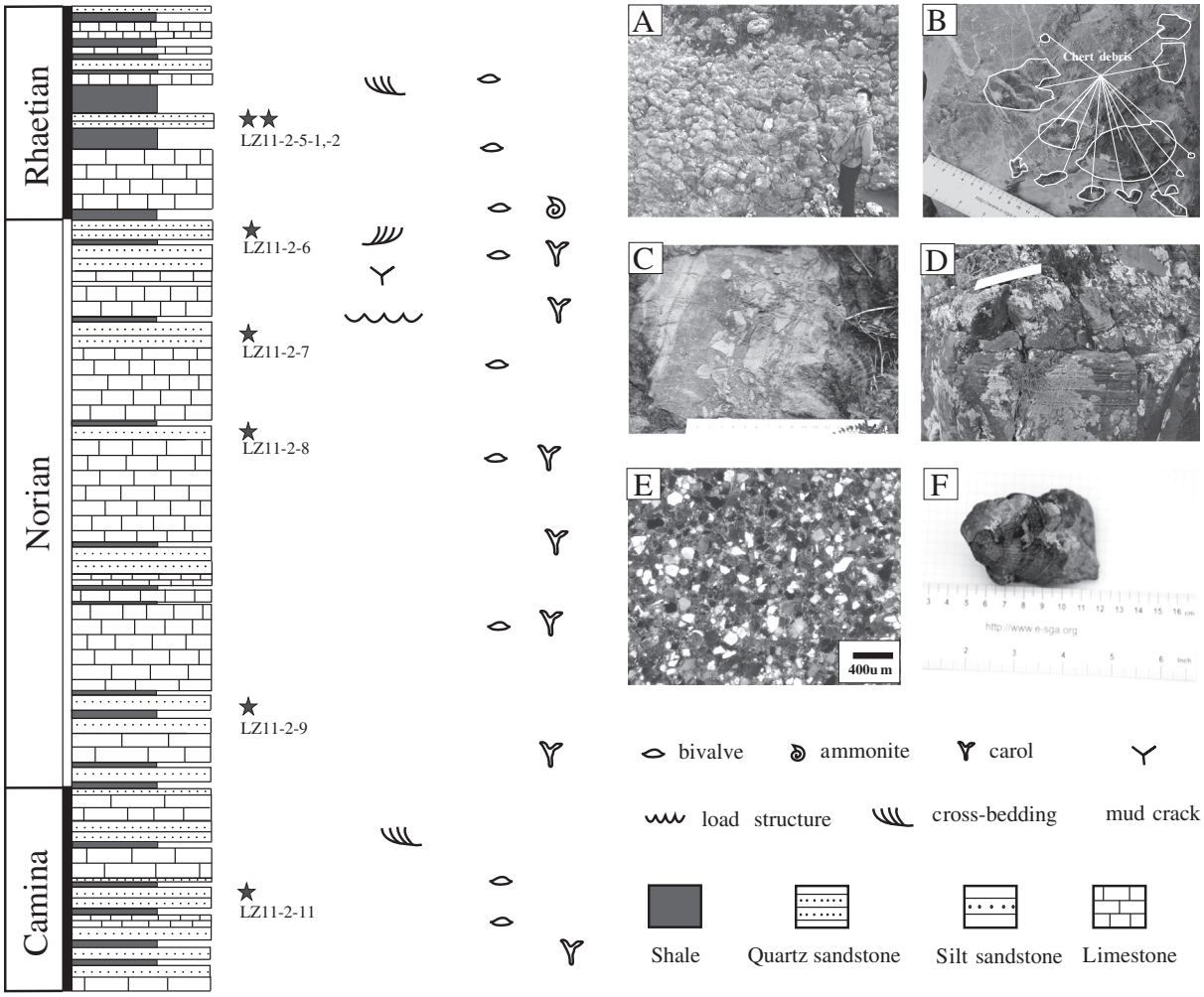

Fig. 2. Sedimentary column of Mailonggang Formation showing the characteristic of lithology, structures and fossils. A. Load structure on the bottom of limestone; B. Chert debris in the limestone; C. Debris flow in the limestone layer; D. Convolute and horizontal bedding in the sandstone; E. Micrograph of the sandstone; F. Coral fossil from the limestone.

Please cite this article as: Li, G., et al., Provenance of Late Triassic sediments in central Lhasa terrane, Tibet and its implication, Gondwana Research (2013), http://dx.doi.org/10.1016/j.gr.2013.06.019

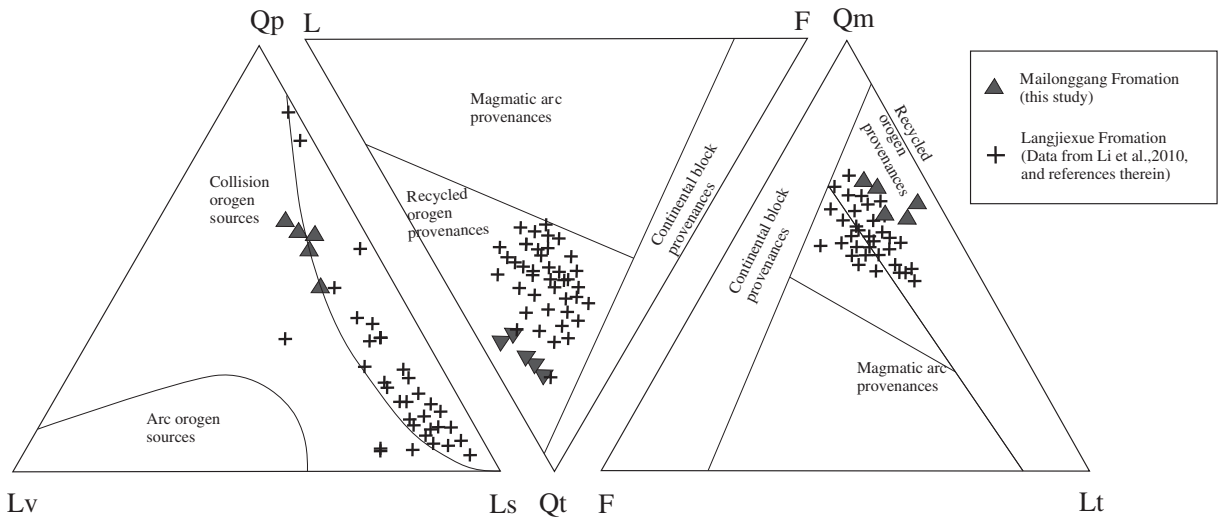

Fig. 3. Sandstone compositions for the Mailonggang Formation: F—feldspar, L—lithic, Lt—total lithics, Ls—sedimentary lithics, Lv—volcanic lithics, Qm—monocrystalline quartz, Qp—polycrystalline quartz, Qt—total quartz. Sandstone samples from this work and previous (Li et al., 2010) plot within the recycled orogen field (fields from Dickinson and Suczek, 1979).

5. Detrital zircon analysis

5.1. Analytical methods

Zircon crystals were obtained from crushed rock using heavy liquid and magnetic separation techniques, and mounted in epoxy resin. Cathodoluminescence (CL) images were used to check the internal structures of individual zircon grains and to select potential target domains for in-situ U–Pb dating and Hf analyses. U–Pb and Hf isotope analyses were conducted at the School of Earth Sciences, University of Melbourne. An Agilent 7500a quadruple inductively-coupled-plasma-mass-spectrometer (QICP-MS), coupled to a 193 nm ArF excimer laser was used to collect U–Pb data, while Hf isotopes were collected by using Nu Plasma Multi Collector-ICPMS, also coupled to a 193 nm ArF excimer laser. Analytical methods followed the procedures outlined in Woodhead et al. (2004, 2007), Eggins et al. (2005), and Paton et al. (2010). The Plesovice, TEMORA and 91500 zircon standards were analyzed along with zircon unknowns to correct of U–Pb fractionation. Data reduction and fractionation correction for U–Pb analyses were undertaken using the Iolite Wavemetrics Igor Pro data analysis software (Hellstrom et al., 2008). Concordia plots were processed using ISOPLOT 3.0 (Ludwig, 2003). The ε_{Hf} and model ages reported here use ^{176}Lu decay constant $\lambda = 1.867 \times 10^{-11} a^{-1}$, $(^{176}Lu/^{177}Hf)_{CHUR} = 0.0332$, $(^{176}Hf/^{177}Hf)_{CHUR,0} = 0.282772$, $(^{176}Lu/^{177}Hf)_{DM} = 0.0332$ and $(^{176}Hf/^{177}Hf)_{DM} = 0.282772$ (Woodhead et al., 2004).

5.2. U–Pb detrital zircon chronology

A total of 517 rounded–subhedral zircon grains with sizes between 50 and 250 μm were analyzed. Cathodoluminescence (CL) images and Th/U ratios show two distinct zircon types. By far the most abundant zircon type (~96%) has strong oscillatory zones and Th/U ratios >0.1 (and up to 5.24) that we interpret to be of a magmatic origin. The high Th/U zircons yielded 493 concordant U–Pb ages (by 90–110%) in the range of 3458–212 Ma, with five major age peaks ~304 Ma, ~560 Ma, ~1155 Ma (three biggest), ~1564 Ma, and ~1750 Ma. The youngest age cluster is in the range of 240–212 Ma (Figs. 4, 5, 6 and Appendix A) and corresponds to a period of significant magmatism in the Lhasa terrane (Li et al., 2003; Zheng et al., 2003; Kapp et al., 2005; Chu et al., 2006; He et al., 2006; K. Liu et al., 2006; Q.X. Liu et al., 2006; Zhang et al., 2007; Zhu et al., 2011, 2013). The second type, comprising only about 4% of the population, is unzoned or only weakly zoned has low Th/U (0.009–0.09), and $^{206}Pb/^{238}U$ ages ranging from 438.7 Ma to 1932.4 Ma. This population probably derives from the metamorphic sources.

5.3. Hf isotopes

A total of 156 grains from the Mailonggang Formation were analyzed for in-situ Hf isotopic abundance. The zircons fall into four broadly defined groups: 1) the youngest group with ages 240–212 Ma has $\varepsilon_{Hf}(t)$ values of −4.2 to +9.4, with T_{DM} ages in the range of ~1008–484 Ma; 2) a group with Paleozoic ages (~512–315 Ma) with $\varepsilon_{Hf}(t)$ values of −16.5 to +8.1 with T_{DM} ages in the range of ~1643–809 Ma; 3) the ~1255–530 Ma group typically has $\varepsilon_{Hf}(t)$ values in the broad range of −31.4 to +11.0 and T_{DM} ages in the range of 2.7–1.1 Ga; and 4) the ~3471–1431 has $\varepsilon_{Hf}(t)$ values in the range of −13.4 to 2.5 and T_{DM} ages of 3.7–1.6 Ga, and a few zircon crystals in this group have more positive $\varepsilon_{Hf}(t)$ values (+4.7 to +9.6) (Fig. 7 and Appendix A).

6. Provenance of the Late Triassic sediments

6.1. Overview of zircon U–Pb ages and Hf isotope data from Lhasa terrane and its relevant terranes

In this section we summarize other zircon U–Pb ages and Hf isotopic data collected from elsewhere in Tibet to help constrain the likely provenance of the Mailonggang Formation (Table 1).

The Qiangtang terrane is located north of Bangong–Nujiang suture zone. Recent detailed geochronologic studies indicate magmatism was active during Paleozoic–Early Mesozoic (~530–202 Ma) (Kapp et al., 2003; Zhai et al., 2007, 2010; Pullen et al., 2011; Zhu et al., 2013). The age distributions of the detrital zircons from the Paleozoic metamorphics exhibit two main peaks at ~524 and ~942 Ma, characterized by $\varepsilon_{Hf}(t)$ values of −37.9 ~ 16.2 and T^{C}_{DM} from 0.7 to 4.0 Ga (Kapp et al., 2003; C.Y. Dong et al., 2011; Zhu et al., 2011).

Lhasa terrane basement rocks (as shown in Fig. 1) have been dated at ~912–501 Ma (Hu et al., 2005; Guynn et al., 2012; Zhu et al., 2013). Late Permian to Early Jurassic magmatic rocks from the central and southern parts of the Lhasa terrane (~265–190 Ma) (Chu et al., 2006; Wen et al., 2008; Ji et al., 2009; Zhu et al., 2009, 2013; references therein, Fig. 1) contain zircons with varying $\varepsilon_{Hf}(t)$ values (−17.3 ~ +16.7) and two-stage Hf model ages (T^{C}_{DM}) from 0.3 to 2.5 Ga (Chu et al., 2006; Zhang et al., 2007; Ji et al., 2009; Zhu et al., 2009, 2011, 2013). Several pre-Permian volcanic central Lhasa terrane sequences have $\varepsilon_{Hf}(t)$ values

Please cite this article as: Li, G., et al., Provenance of Late Triassic sediments in central Lhasa terrane, Tibet and its implication, Gondwana Research (2013), http://dx.doi.org/10.1016/j.gr.2013.06.019

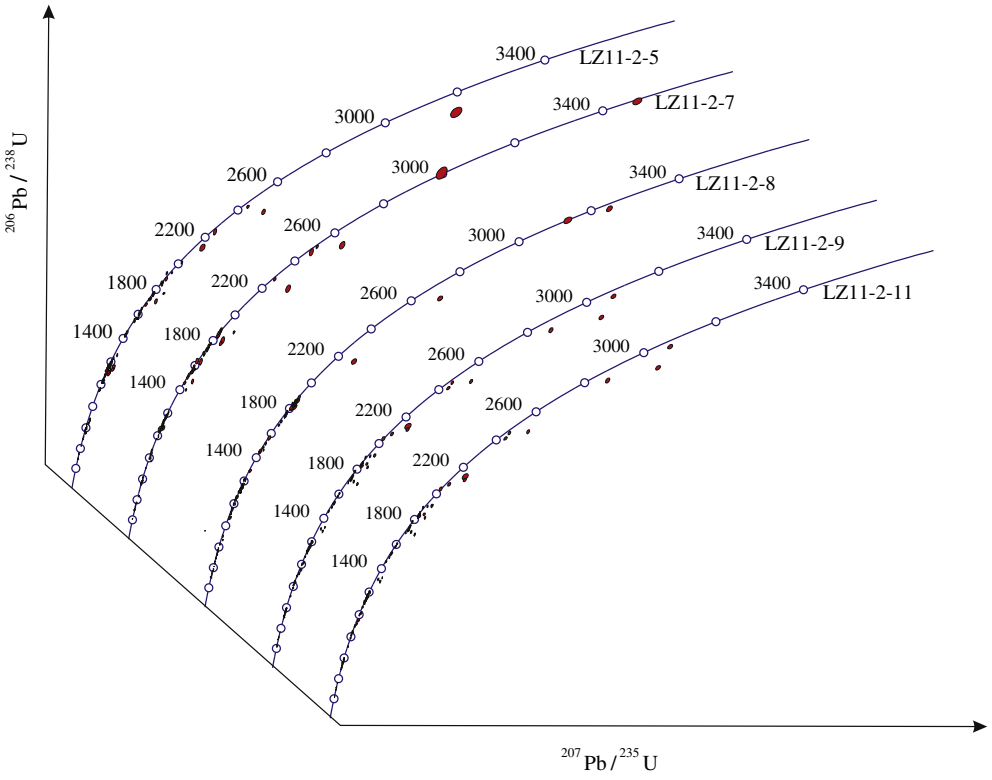

Fig. 4. U–Pb concordia plots for detrital zircon analyses from the Upper Triassic Mailonggang Formation.

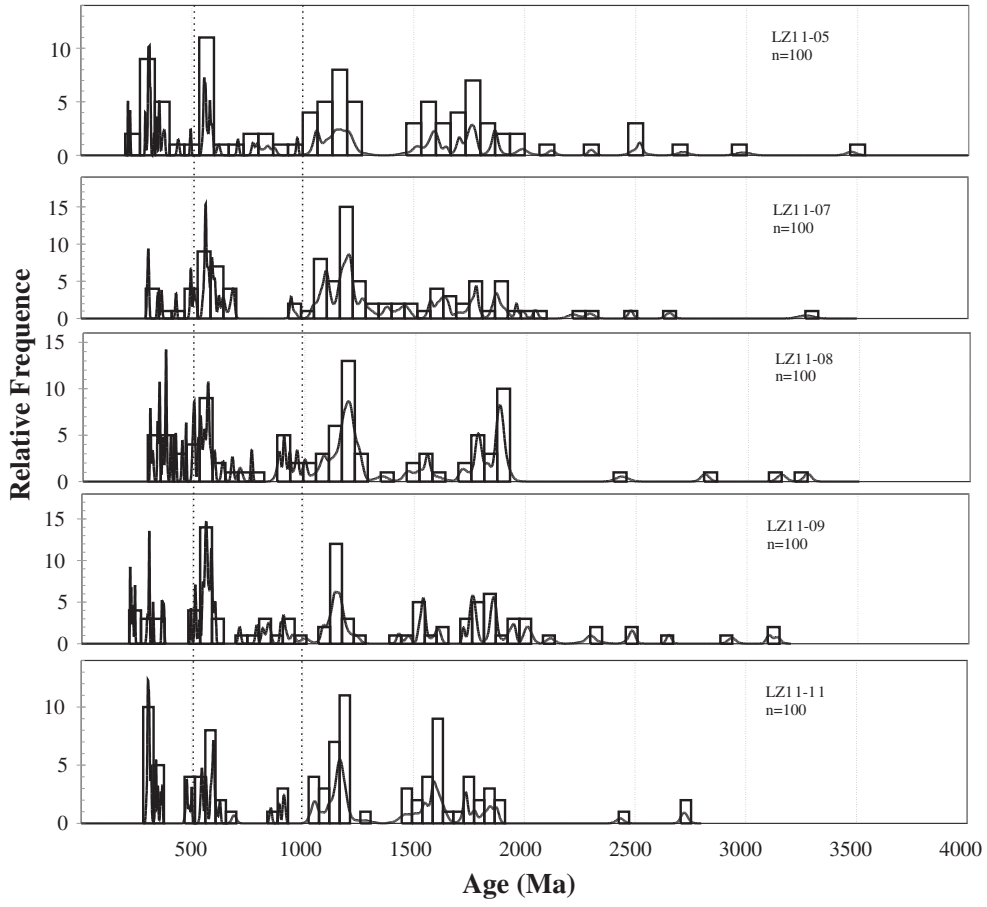

Fig. 5. U–Pb age probability plots for detrital zircon analyses from the Mailonggang Formation.

Please cite this article as: Li, G., et al., Provenance of Late Triassic sediments in central Lhasa terrane, Tibet and its implication, Gondwana Research (2013), http://dx.doi.org/10.1016/j.gr.2013.06.019

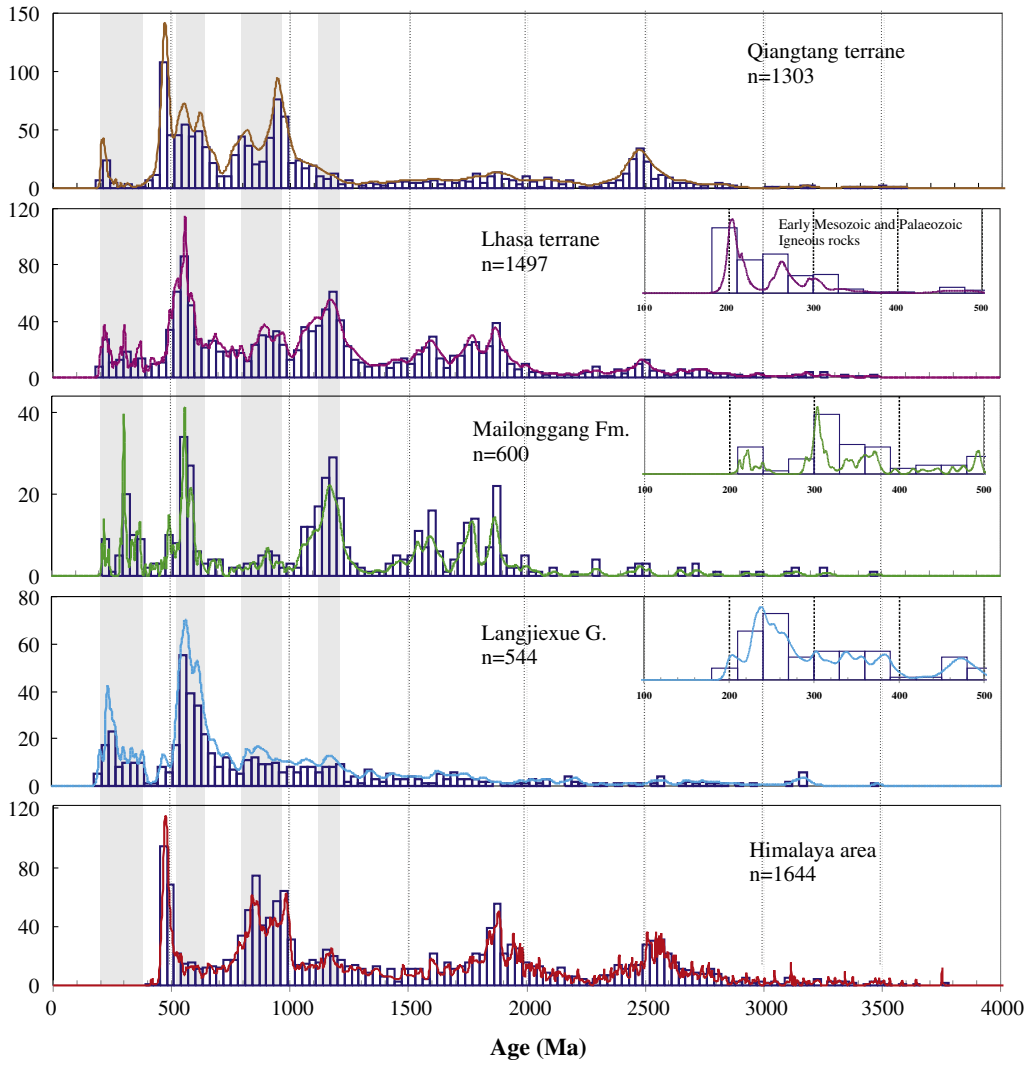

Fig. 6. Pre-Jurassic detrital zircon age distributions of Mailonggang Formation and relevant databases. Data sources (see Table 1): Qiangtang (C.Y. Dong et al., 2011; Pullen et al., 2011; Zhu et al., 2011); Lhasa (Leier et al., 2007; Pullen et al., 2008; Wu et al., 2010; Zhu et al., 2011); Igneous rocks in the Lhasa terrane (Chu et al., 2006; Zhang et al., 2007; Chen et al., 2008; Ji et al., 2009; Zhu et al., 2009, 2011; Li et al., 2012); Langjiexue Group (Aikman et al., 2008; Li et al., 2010); Himalaya (DeCelles et al., 2004; Gehrels et al., 2006; Myrow et al., 2010; Zhu et al., 2011).

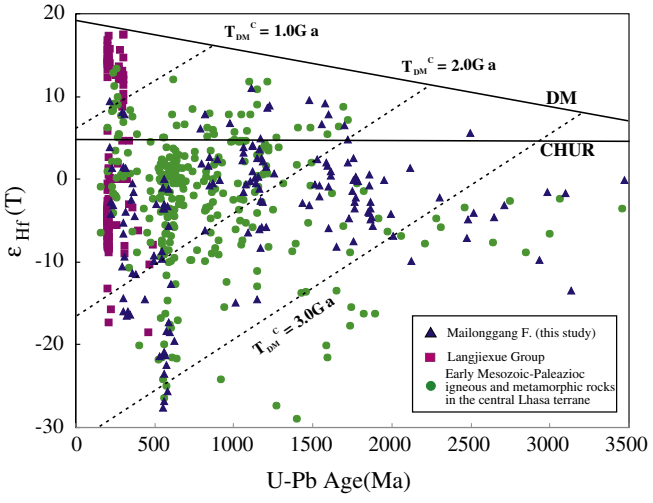

Fig. 7. A plot of U–Pb detrital ages vs $\varepsilon_{Hf}(t)$ values of the detrital zircon from the Mailonggang Formation and Langjiexue Group, and crystallized zircon from igneous rocks in central Lhasa terrane. Data from previous works include: from the Langjiexue Group (Li et al., 2010); from the central Lhasa terrane igneous and metamorphic rocks (Chu et al., 2006; Zhang et al., 2007; Chen et al., 2008; Ji et al., 2009; Zhu et al., 2009, 2011).

in range of −13.9 ~ +7.5 with T^{C}_{DM} values ranging from 0.9 to 2.3 Ga (Dong et al., 2010; Zhu et al., 2013). X. Dong et al. (2011) reported the U–Pb zircon ages of ~225–212 Ma indicated the metamorphic event occurred in Nyainqentagnlha during Triassic near this study region. In the southern Lhasa terrane, Early Jurassic volcanic rocks (both felsic and mafic, with minor amounts of andesite) in the Yeba Formation dated at ~190–172 Ma (Zhu et al., 2008). Pre-Mesozoic inherited zircons and detrital zircons are common in Lhasa, showing $\varepsilon_{Hf}(t)$ values in range of −38.1 ~ +15.6 with T^{C}_{DM} ages ranging from 0.3 to 3.9 Ga (Chu et al., 2006; Leier et al., 2007; Ji et al., 2009; Wu et al., 2010; Zhu et al., 2011).

To the south of the Indus–Yarlung suture zone, crystalline basement outcrops in the Greater Himalaya (dominantly Precambrian in age) and in the Tethyan Himalaya as a series of the discontinuous belt of gneiss domes with U–Pb ages of about 500 Ma (Lee et al., 2000; Decelles et al., 2004; Gehrels et al., 2006; Quigley et al., 2008; Myrow et al., 2010). The Paleozoic magmatic rocks are reported in Greater Himalaya (Zanskar, Mandi, Yadong, Abor), and Tethyan Himalaya (Gyirong, Selong, Kangmar, Mabja) (Spring et al., 1993; Garzanti et al., 1999; Miller et al., 2001; Cawood et al., 2007; Zhu et al., 2010). Detrital zircons from the Permian–Precambrian clastic strata in these region have four major age peaks at ~540, ~950, ~1500–1700 Ma, and 2500 Ma and have a wide range of $\varepsilon_{Hf}(t)$ values (−29.5 ~ 12.6) with varying T^{C}_{DM}

Please cite this article as: Li, G., et al., Provenance of Late Triassic sediments in central Lhasa terrane, Tibet and its implication, Gondwana Research (2013), http://dx.doi.org/10.1016/j.gr.2013.06.019

Table 1
Zircon U–Pb ages (pre-Jurrasic) and Hf isotopic data from potential sources or relevant units for the Late Triassic sequences.

Potential sources/relevant units	Age/Ma	$\varepsilon_{Hf}(t)$	$T^{C}_{DM(Hf)}$/Ga	References
Qiangtang				
Basement	~476 to 471	Lack	Lack	C.Y. Dong et al. (2011), Pullen et al. (2011), Zhai et al. (2007, 2010), Zhu et al. (2011, 2013);
Igneous rocks	~530 to 202	−37.9 ~ +16.2	4.0–0.7	
Inherited and detrital zircons	~3596 to 408	−37.8 ~ 23.5	3.7–0.7	
Lhasa				
Basement	~912 to 501(mainly ~500)	Lack	Lack	Chen et al. (2008), Chu et al. (2006, 2011), Dong et al. (2010), X. Dong et al. (2011), Guynn et al. (2012), Hu et al. (2005), Ji et al. (2009), Leier et al. (2007), Pullen et al. (2008), Wu et al. (2010), Zhang et al. (2007), Zhu et al. (2009, 2011, 2013);
Igneous rocks	~546 to 200	−17.3 ~ +16.7	2.3–0.25	
Inherited detrital zircon	~3602 to 200	−38.1 ~ +15.6	3.9–0.3	
Yarlung Zangbo melange zone				
Detrital zircon (Tr3)	~3454 to 201	−40.3 ~ +13.4	3.9–0.4	Aikman et al. (2008), Li et al. (2010);
Himalaya				
Basement	~970 to 470 (mainly ~500)	Lack	Lack	DeCelles et al. (2004), Gehrels et al. (2006), Hu et al. (2010), Myrow et al. (2010), Zhu et al. (2011).
Inherited and detrital zircons	~3523 to 470	−29.5 ~ 12.6	3.7–1.0	

ages (3.7–1.0 Ga) (Decelles et al., 2004; Myrow et al., 2010; Zhu et al., 2011). In the Indus–Yarlung melange zone, the Triassic Langjiexue Group shows different detrital zircon age patterns compared to those obtained from the Tethyan Himalaya sediments, with a distinct Late Paleozoic to Early Mesozoic (~358–224 Ma) age peak and with $\varepsilon_{Hf}(t)$ values of −3.5 ~ +13.5 (most positive) and T^{C}_{DM} ages ranging from ~1.6 Ga to 443 Ma (Li et al., 2010).

6.2. General provenance considerations

Detrital zircon ages of the samples from Mailonggang Formation include major Paleozoic, Late Neoproterozoic, Late Mesoproterozoic peaks and a broad distribution of Early Neoproterozoic–Early Paleoproterozoic. This range of zircon ages is common in all Tibet terranes (Qiangtang, Lhasa, and Himalaya). However, there are some important differences among these terranes, For example, the major Precambrian age peaks in the Qiangtang terrane occur at ~ 550 Ma, ~800 Ma, ~950 Ma, and ~2500 Ma. For the Lhasa terrane the main peaks are at ~550 and ~1170 Ma while for the Himalaya, age peaks are at ~480, ~840, and ~950 Ma (Fig. 6).

The absence of significant detrital zircons in the Mailonggang Formation with age peaks of ~800, ~950 Ma and ~2500 Ma precludes a Qiangtang terrane provenance as the main source for Mailonggang Formation (Fig. 6). Furthermore, the immature nature of the Mailonggang sandstone also suggests a proximal source. Lastly, paleogeographic constraints also argue against the possibility that the Mailonggang sediments were derived from the Qiangtang terrane, since there is evidence that Qiangtang terrane was not juxtaposed with the Lhasa terrane until Late Jurassic or Early Cretaceous (Allègre et al., 1984; Yin and Harrison, 2000; Zhu et al., 2013; references therein).

Similarly, a Himalayan provenance can be precluded mainly because of the paleogeographic constraints. The existence of a Late Triassic deep water flysch (Langjiexue Group) in IYSZ deposited between Lhasa and Himalayan terranes (Fig. 1; Yin, 2006) would seemingly preclude an obvious route for Himalayan sediments to be transported to the shallow water carbonate–clastic platforms in the Lhasa terrane from south to north. Furthermore, measured paleocurrents in Langjiexue Group show a southward paleoflow direction (Li et al., 2004), which also indicates that the sediments of Himalaya didn't reach into the Lhasa terrane to the north.

The youngest cluster of U–Pb zircon ages (~240–212 Ma) with $\varepsilon_{Hf}(t)$ values of −4.2 to +9.4 from the Mailonggang Fm. are compatible with the derivation of the Lhasa terrane and Triassic Gangdese magmatic arc rocks (Figs. 1, 6, 7), while parts of the negative $\varepsilon_{Hf}(t)$ zircons could derive from the metamorphic rocks (C.Y. Dong et al., 2011; X. Dong et al., 2011), and/or from the southern Lhasa terrane as well (Zhu et al., 2013). Parts of the Paleozoic zircons are comparable to the Permian and pre-Permian volcanic occurrences in the central Lhasa terrane with $\varepsilon_{Hf}(t)$ values in range of −13.9 ~ +7.5 (Zhu et al., 2011). The distribution of Paleozoic zircons in this study with two main peaks at ~550 and ~1170 Ma is consistent with the patterns of the detrital zircons with the varied $\varepsilon_{Hf}(t)$ values (−38.1 ~ 15.6) and T^{C}_{DM} age (~0.3 to ~3.9 Ga) from Permo-Carboniferous sandstones in the central Lhasa terrane (Leier et al., 2007; Pullen et al., 2008; Zhu et al., 2011; Figs. 5, 6). These indicate the igneous, recycled sedimentary and a bit of metamorphic rocks in central Lhasa terrane provided the sources, which quite accords with the results of petrography and heavy mineral analysis.

Our new zircon data, combined with petrography and heavy mineral analysis, indicate the proximal igneous rocks, recycled sediments and some ultramafic, metamorphic rocks are the mainly potential sources for the Mailonggang Formation. These sources match with the rock units in the central Lhasa terrane and the Sumdo–Cuoqen belt (Fig. 1). Meanwhile, the Sumdo–Cuoqen belt has been initially defined as a new Late Permian–Triassic orogenic belt in the central Lhasa terrane, indicated by the Late Paleozoic high or ultrahigh metamorphic belt with igneous rocks and Early Mesozoic thrust fault system (Chen et al., 2009; Li et al., 2009; Yang et al., 2009; Li et al., 2011; X. Dong et al., 2011). The Mailonggang sequence is in depositional contact with or located immediately southeast of the Sumdo area. Generally, according to these evidences and our results, we suggest the Upper Triassic Mailonggang Formation was derived from the Late Permian–Triassic orogenic belt along Sumdo–Cuoqen belt in central Lhasa terrrane.

7. Discussion

One issue concerns the relationship between the Upper Triassic Mailonggang Formation and the Langjiexue Group. Li et al. (2010) proposed that the Triassic Langjiexue Group on the south side of Indus–Yarlung ophiolites (Fig. 1) originated along the southern margin of the Lhasa terrane in a forearc or backarc setting (Li et al., 2010). Our analysis suggests that both the Mailonggang and Langjiexue sequences were likely derived from the Late Permian–Triassic Sumdo–Cuoqen belt in the Lhasa terrane. This contention is supported by the similarities in detrital zircon ages with Hf isotope signatures and especially large peaks in Late Paleozoic and ~550 Ma (Figs. 5, 6). These signatures preclude Himalayan sources but are consistent with the Permian–Triassic age igneous rocks reported in the Lhasa terrane (Li et al., 2010; Figs. 1, 6). Furthermore, both formations share petrographic similarities distinctive of recycled orogen affinity (Fig. 3; Li et al., 2004, 2010) and are characterized by similar heavy mineral assemblages (L.S. Zeng et al., 2009; Q.G. Zeng et al., 2009). In the Langjiexue Group, paleocurrent indicators imply a northerly source (Li et al., 2004; Li et al., 2010), while Nd isotopic compositions are also consistent with derivation from the Lhasa terrane (Dai et al., 2008). Finally, a recent interpretation (K. Liu et al., 2006; Q.X. Liu et al., 2006) of the INDEPTH seismic profiling of Zhao and

Please cite this article as: Li, G., et al., Provenance of Late Triassic sediments in central Lhasa terrane, Tibet and its implication, Gondwana Research (2013), http://dx.doi.org/10.1016/j.gr.2013.06.019

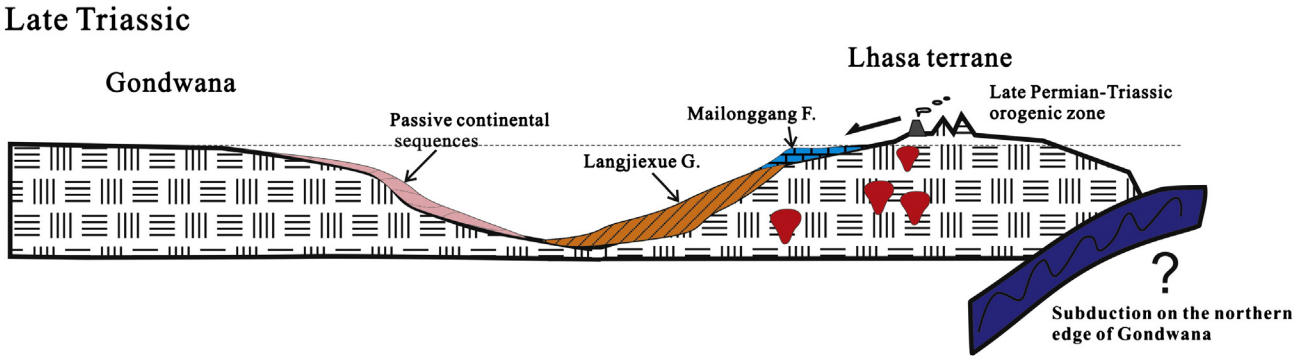

Fig. 8. The sketch tectonic model of the Upper Triassic sequences on the south margin of the Lhasa terrane.

Nelson (1993) has the northern margin of Indian block extending no further north than the Main Himalayan Thrust (MHT) along the south margin of the Langjiexue Group, rather than all the way to the IYSZ. The K. Liu's et al. (2006), Q.X. Liu's et al. (2006) interpretation is consistent with the notion that Langjiexue Group is part of the Lhasa terrane. We conclude that the Langjiexue Group and Mailonggang Formation were likely both deposited on the south margin of Lhasa terrane (Fig. 8) probably before the initial drifting of Lhasa terrane from Gondwana. As mentioned earlier, the newly recognized Late Permian–Triassic orogenic belt in the central Lhasa terrane exhibits Mid–Late Triassic cooling ages. We propose that the erosional denudation of this belt provided the proximal source of immature terrigenous sediment observed both in the Mailonggang Formation and the Langjiexue Group.

A key question is whether the Lhasa terrane originally derives from the Indian (e.g., Allègre et al., 1984; Yin and Harrison, 2000) or Australian sector of the Gondwana margin (Zhu et al., 2011, 2013). In the former case, a simple model for the early evolution of Neo-Tethys sees the Lhasa terrane rifted from India along the southern edge of Lhasa terrane, thereby segmenting the formerly contiguous Langjiexue Group and Mailonggang Formation during Late Triassic–Early Jurassic period. In this scenario, the Lhasa terrane subsequently collided with the Qiangtang Terrane in the Early Cretaceous (Yin and Harrison, 2000; Yin, 2006). A key observation supporting this hypothesis is the presence of rift-related Late Triassic–Early Jurassic magmatism in the Lhasa terrane (Zhang et al., 2007; Zhu et al., 2013), which indicates that rifting had continued well after the Permian (Garzanti et al., 1999; Chauvet et al., 2008). Similar ages and styles of magmatism are observed along Gondwanan margin fragment in East Indonesia (Java), New Guinea and Northeast Australia as a precursor to eventual Jurassic breakup (Crowhurst et al., 2004; Hill and Hall, 2003; Metcalfe, 2011; Van Wyck and Williams, 2002). The alternative hypothesis of Zhu et al. (2011, 2013), which proposes that the Lhasa terrane derives from the Australian margin necessarily involves a more complex paleogepgraphic circuit for the Lhasa terrane. Our new data do not directly discriminate these two hypotheses, though the detrital zircon age distributions in the sediments show the differences between Lhasa terrane and Himalaya (part of Indian block), which is similar to the previous results (Li et al., 2010; Zhu et al., 2013).

Acknowledgments

We are grateful to Prof. Woodhead J. and Greg A. for helping with zircon U–Pb and Hf isotope experiments. We thank Dr. Steven Boger, Prof. Guochun Zhao and two anonymous reviewers for their insightful and patient comments that helped improve this study. This study benefited from financial support by Geological Survey of China (No.1212010818094) and Australia research council DECRA (Discovery Early Career Research Award, DE120102245).

Appendix A. Supplementary data

Supplementary data to this article can be found online at http://dx.doi.org/10.1016/j.gr.2013.06.019.

References

Aikman, A.B., Harrison, T.M., Ding, L., 2008. Evidence for Early (>44 Ma) Himalayan crustal thickening, Tethyan Himalaya, southeastern Tibet. Earth and Planetary Science Letters 274, 14–23.

Aitchison, J.C., Ali, J.R., Davis, A.M., 2007. When and where did India and Asia collide? Journal of Geophysical Research 112, B05423.

Allègre, C.J., Courtillot, V., Tapponnier, P., et al., 1984. Structure and evolution of the Himalaya–Tibet orogenic belt. Nature 307, 17–22.

Cai, F., Ding, L., Leary, R.J., Wang, H.Q., Xu, Q., Zhang, L.Y., Yue, Y.H., 2012. Tectonostratigraphy and provenance of an accretionary complex within the Yarlung–Zangpo suture zone, southern Tibet: Insights into subduction–accretion processes in the Neo-Tethys. Tectonophysics 574–575, 181–192.

Cawood, P.A., Johnson, M.R.W., Nemchin, A.A., 2007. Early Palaeozoic orogenesis along the Indian margin of Gondwana: tectonic response to Gondwana assembly. Earth and Planetary Science Letters 255, 70–84.

Chauvet, F., Lapierre, H., Bosch, D., Guillot, S., Mascle, G., Vannay, J.C., Cotton, J., Brunet, P., Keller, F., 2008. Geochemistry of the Panjal Trap basalts (NW Himalaya): records of the Pangea Permian break-up. Bulletin de la Societe Geologique de France 179 (4), 383–395.

Chen, S.Y., Yang, J.S., Xu, X.Z., Li, H.Q., Yang, Y.H., 2008. Study of Lu–Hf geochemical tracing and LA-ICPMS U–Pb isotopic dating of the Sumdo eclogite from the Lhasa block, Tibet. Acta Petrologica Sinica 24 (7), 1528–1538 (Chinese with English abstract).

Chen, S.Y., Yang, J.S., Li, Y., Xu, X.Z., 2009. Ultramafic terranes in Sumdo region, Lhasa terrane, eastern Tibet Plateau: an ophiolite unit. Journal of Earth Science 20, 332–347.

Chu, M.F., Chung, S.L., Song, B., Liu, D.Y., O'Reilly, S.Y., Pearson, N.J., Ji, J.Q., Wen, D.J., 2006. Zircon U-Pb and Hf isotope constraints on the Mesozoic tectonics and crustal evolution of southern Tibet. Geology 34 (9), 745–748.

Chu, M.F., Chung, S.L., O'Reilly, S.Y., Pearson, N.J., Wu, F.Y., Li, X.H., Ji, J.Q., Liu, D.Y., Ji, J.Q., Chu, C.H., Lee, H.Y., 2011. India's hidden inputs to Tibetan orogeny revealed by Hf isotopes of Transhimalayan zircons and host rocks. Earth and Planetary Science Letters 307, 479–486.

Crowhurst, P.V., Maas, R., Hill, K.C., Foster, D.A., Fanning, C.M., 2004. Isotopic constraints on crustal architecture and Permo-Triassic tectonics in New Guinea: possible links with eastern Australia. Australian Journal of Earth Sciences 51 (1), 109–124.

Dai, J.G., Yin, A., Liu, W.C., Wang, C.S., 2008. Nd isotopic compositions of the Tethyan Himalayan Sequence in southeastern Tibet. Science in China Series D: Earth Sciences 51 (9), 1306–1316.

DeCelles, P., Gehrels, G., Najman, Y., Martin, A.J., Carter, A., Garzanti, E., 2004. Detrital geochronology and geochemistry of Cretaceous–Early Miocene strata of Nepal: implications for timing and diachroneity of initial Himalayan orogenesis. Earth and Planetary Science Letters 227 (3), 313–330.

Dewey, J.F., Shackleton, R.M., Chang, C.F., Sun, Y.Y., 1988. The tectonic evolution of the Tibetan Plateau. Philosophical Transactions of the Royal Society of London (Series A): Mathematical and Physical Sciences 327, 379–413.

Dickinson, W.R., Suczek, C.A., 1979. Plate tectonics and sandstone composition. AAPG Bulletin 63 (12), 2164–2182.

Ding, L., Kapp, P., Wan, X., 2005. Palaeocene–Eocene record of ophiolite obduction and initial India–Asia collision, south-central Tibet. Tectonics 24, TC3001. http://dx.doi.org/10.1029/2004TC001729.

Dong, X., Zhang, Z.M., Geng, G.S., Liu, F., Wang, W., Yu, F., 2010. Devonian magmatism from the southern Lhasa terrane, Tibetan Plateau. Acta Petrologica Sinica 26, 2226–2232 (in Chinese with English abstract).

Dong, C.Y., Li, C., Wan, Y.S., Wang, W., Wu, Y.W., Xie, H.Q., Liu, D.Y., 2011. Detrital zircon age model of Ordovician Wenquan quartzite south of Lungmuco–Shuanghu suture in the Qiangtang area, Tibet: constraint on tectonic affinity and source regions. Science China Earth Sciences 54 (7), 1034–1042.

Dong, X., Zhang, Z.M., Liu, F., Wang, W., Yu, F., Shen, K., 2011. Zircon U–Pb geochronology of the Nyainqêntanglha Group from the Lhasa terrane: new constraints on the Triassic orogeny of the south Tibet. Journal of Asian Earth Sciences 42, 732–739.

Eggins, S.M., Grün, R., McCulloch, M.T., Pike, A.W.G., Chappell, J., Kinsley, L., Mortimer, G., Shelley, M., Murray-Wallace, C.V., Spötl, C., 2005. In situ U-series dating by laser-ablation multi-collector ICPMS: new prospects for Quaternary geochronology. Quaternary Science Reviews 24, 2523–2538. http://dx.doi.org/10.1016/j.quascirev.2005.07.006.

England, P.C., Searle, M.A., 1986. Cretaceous–Tertiary deformation of the Lhasa terrane and its implications for crustal thickening in Tibet. Tectonics 5, 1–14.

Garzanti, E., Le Fort, P., Sciunnach, D., 1999. First report of Lower Permian basalts in South Tibet: tholeiitic magmatism during break-up and incipient opening of Neotethys. Journal of Asian Earth Sciences 17, 533–546.

Gehrels, G.E., DeCelles, P.G., Ojha, T.P., Upreti, B.N., 2006. Geologic and U–Th–Pb geochronologic evidence for early Palaeozoic tectonism in the Kathmandu thrust sheet, central Nepal Himalaya. Geological Society of America Bulletin 118, 185–198.

Geng, Q.R., Wang, L.Q., Pan, G.T., Jin, Z.J., Zhu, D., Liao, Z.L., Li, G.M., Li, F.Q., 2007. Volcanic rock geochemistry and tectonic implication of the Luobadui Formation on the Gangdese zone, Xizang (Tibet). Acta Petrologica Sinica 23 (11), 2699–2714 (Chinese with English abstract).

Guynn, J., Kapp, P., Gehrels, G., Ding, L., 2012. U–Pb geochronology 1 of basement rocks in central Tibet and palaeogeographic implications. Journal of Asian Earth Sciences 43, 23–50.

He, Z.H., Yang, D.M., Zheng, C.Q., Wang, T.W., 2006. Isotopic dating of the Mamba granitoid in the Gangdise tectonic belt and its constraint on the subduction time of the Neotethys. Geological Review 52 (1), 100–106 (Chinese with English Abstract).

Hellstrom, J., Paton, C., Woodhead, J., Hergt, J., 2008. Iolite: software for spatially resolved LA-(quad and MC) ICPMS analysis. In: Sylvester, P. (Ed.), Laser Ablation ICP-MS in the Earth Sciences: Current Practices and Outstanding Issues. Mineralogical Association of Canada, Quebec, Canada, pp. 343–348.

Hill, K.C., Hall, R., 2003. Mesozoic–Cenozoic evolution of Australia's New Guinea margin in a west Pacific context. Geological Society of America Special Paper 372, 265–290.

Hu, D.G., Wu, Z.H., Jiang, W., Shi, Y.R., Ye, P.S., Liu, Q.S., 2005. SHRIMP zircon U–Pb age and Nd isotopic study on the Nyainqêntanglha Group in Tibet. Science in China Series D: Earth Sciences 48, 1377–1386.

Hu, X.L., Jansa, L., Chen, L., Griffin, W.L., O'Reilly, S.Y., Wang, J.G., 2010. Provenance of Lower Cretaceous Wölong Volcaniclastics in the Tibetan Tethyan Himalaya: implications for the final breakup of Eastern Gondwana. Sedimentary Geology 223 (3–4), 193–205.

Ji, Z.S., Yao, J.X., Yang, X.D., Zang, W.S., Wu, G.C., 2003. Conodont zonations of Norian in Lhasa area, Xizang (Tibet) and their global correlation. Acta Palaeontologica Sinica 42 (3), 382–392 (Chinese with English abstract).

Ji, W.Q., Wu, F.Y., Chung, S.L., Li, J.X., Liu, C.Z., 2009. Zircon U–Pb chronology and Hf isotopic constraints on the petrogenesis of Gangdese batholiths, southern Tibet. Chemical Geology 262, 229–245.

Kapp, P., Murphy, M.A., Yin, A., Harrison, T.M., Ding, L., Guo, J.R., 2003. Mesozoic and Cenozoic tectonic evolution of the Shiquanhe area of western Tibet. Tectonics 22, 1029. http://dx.doi.org/10.1029/2001 TC001332.

Kapp, J.L.D., Harrison, T.M., Kapp, P., Grove, M., Lovera, O.M., Ding, L., 2005. The Nyainqentanglha Shan: a window into the tectonic, thermal, and geochemical evolution of the Lhasa terrane, southern Tibet. Journal of Geophysical Research 110, B08413. http://dx.doi.org/10.1029/2004JB003330.

Kapp, P., DeCelles, P.G., Leier, A.L., Fabijanic, J.M., He, S., Pullen, A., Gehrels, G.E., Ding, L., 2007. The Gangdese retroarc thrust belt revealed. GSA Today 17 (7), 4–9.

Lee, J., Hacker, B.R., Dinklage, W.S., Wang, Y., Gans, P., Calvert, A., Wan, J., Chen, W., Blythe, A.E., McClelland, W., 2000. Evolution of the Kangmar dome, southern Tibet: structural, petrologic, and thermochronologic constraints. Tectonics 19, 872–895.

Leier, A.L., Kapp, P., Gehrels, G.E., DeCelles, P.G., 2007. Detrital zircon geochronology of Carboniferous–Cretaceous strata in the Lhasa Terrane, Southern Tibet. Basin Research 19, 361–378.

Li, H.D., 1990. Report of Regional Geological Survey in Xigaze (1/200 000). Geological Publishing House, Beijing (in Chinese).

Li, C., Wang, T.W., Li, H.M., Zeng, Q.G., 2003. Discovery of Indosinian megaporphyritic granodiorite in the Gangdise area: evidence for the existence of Palaeo-Gangdise. Geological Bulletin of China 22 (5), 364–366 (Chinese with English abstract).

Li, X.H., Zeng, Q.G., Wang, C.S., Xie, Y.W., 2004. Provenance analysis of the Upper Triassic Langjiexue Group in the Southern Tibet, China. Acta Sedimentologica Sinica 22 (4), 553–559 (in Chinese with English abstract).

Li, G.W., Liu, X.H., Pullen, A., Wei, L.J., Liu, X.B., Huang, F.X., Zhou, X.J., 2010. In-situ detrital zircon geochronology and Hf isotopic analyses from Upper Triassic. Earth and Planetary Science Letters 297, 461–470.

Li, H.Q., Xu, Z.Q., Yang, J.S., Cai, Z.H., Chen, S.Y., Tang, Z.M., 2009. Records of Indosinian orogenesis in Lhasa terrane, Tibet. Journal of Earth Science 20 (2), 348–363. http://dx.doi.org/10.1007/s12583-009-0029-9.

Li, H.Q., Xu, Z.Q., Yang, J.S., Tang, Z.M., Yang, M., 2011. Syn-collisional exhumation of Sumdo eclogite in the Lhasa Terrane, Tibet: Evidences from structural deformation and ^{40}Ar–^{39}Ar geochronology. Earth Science Frontiers 18 (3), 66–78 (Chinese with English abstract).

Li, F.Q., Liu, W., Wang, B.D., Zhang, S.Z., 2012. The continuation of the subduction of Palaeo-Tethys Ocean within Lhasa terrane in Early-Middle Triassic: evidence from volcanic rocks and HP Metamorphic rocks. Acta Petrologica et Mineralogica 31 (2), 119–132 (Chinese with English Abstract).

Liu, K., Zhao, W.J., Jiang, W., Wu, Z.H., 2006. Where is the north margin of Indian terrane? Geological Bulletin of China 25 (1–2), 43–47 (Chinese with English Abstract).

Liu, Q.X., Jiang, W., Jian, P., Ye, P.S., Wu, Z.H., Hu, D.G., 2006. Zircon SHRIMP U–Pb age and petrochemical and geochemical features of Mesozoic muscovite monzonitic granite at Ningzhong, Tibet. Acta Petrologica Sinica 22 (3), 643–652 (Chinese with English Abstract).

Liu, X.H., Ju, Y.T., Wei, L.J., Li, G.W., 2010. An alternative tectonic model for the Yarlung Zangbo suture zone. Science in China Series D 53 (1), 448–463.

Liu, X.H., Hsu, J.H., Ju, Y.T., Li, G.W., Liu, X.B., Wei, L.J., Zhou, X.J., Zhang, X.G., 2012. New interpretation of tectonic model in south Tibet. Journal of Asian Earth Sciences 56, 147–159.

Ludwig, K.R., 2003. User's manual for isoplot 3.0: a geochronological toolkit for Microsoft Excel. Special Publication, 4. Berkeley Geochronology Center.

Metcalfe, I., 2011. Tectonic framework and Phanerozoic evolution of Sundaland. Gondwana Research 19 (1), 3–21.

Miller, C., Thöni, M., Frank, W., Grasemann, B., Klötzi, U., Guntli, P., Draganits, E., 2001. The Early Palaeozoic magmatic event in the Northwest Himalaya: source, tectonic setting and age of emplacement. Geological Magazine 138, 237–251. http://dx.doi.org/10.1017/S0016756801005283.

Mo, X.X., Hou, Z.Q., Niu, Y.L., Dong, G.C., Qu, X.M., Zhao, Z.D., Yang, Z.M., 2007. Mantle contributions to crustal thickening during continental collision: evidence from Cenozoic igneous rocks in southern Tibet. Lithos 96, 225–242.

Molnar, P., Tapponnier, P., 1975. Cenozoic tectonics of Asia: effects of a continental collision. Science 189, 419–426.

Morton, A.C., Hallsworth, C.R., 1994. Identifying provenance-specific features of detrital heavy mineral assemblages in sandstones. Sedimentary Geology 90 (3), 241–256.

Myrow, P.M., Hughes, N.C., Goodge, J.W., Fanning, C.M., Williams, I.S., Pengm, S.C., Bhargava, O.N., Parcha, S.K., Pogue, K.R., 2010. Extraordinary transport and mixing of sediment across Himalayan central Gondwana during the Cambrian–Ordovician. Geological Society of America Bulletin 122, 1660–1670.

Pan, G.T., Mo, X.X., Hou, Z.Q., Zhu, D.C., Wang, L.Q., Li, G.M., Zhao, Z.D., Geng, Q.R., Liao, Z.L., 2006. Spatial–temporal framework of the Gangdese orogenic belt and its evolution. Acta Petrologica Sinica 22, 521–533 (Chinese with English abstract).

Paton, C., Woodhead, J.D., Hellstrom, J.C., Hergt, J.M., Greig, A., Maas, R., 2010. Improved laser ablation U–Pb zircon geochronology through robust downhole fractionation correction. Geochemistry, Geophysics, Geosystems 11, Q0AA06. http://dx.doi.org/10.1029/2009G C002618.

Pullen, A., Kapp, P., Gehrels, G.E., DeCelles, P.G., Brown, E.H., Fabijanic, J.M., Ding, L., 2008. Gangdese retroarc thrust belt and foreland basin deposits in the Damxung area, southern Tibet. Journal of Asian Earth Sciences 33 (5), 323–336.

Pullen, A., Kapp, P., Gehrels, G.E., Ding, L., Zhang, Q.H., 2011. Metamorphic rocks in central Tibet: lateral variations and implications for crustal structure. Geological Society of America Bulletin 123, 585–600. http://dx.doi.org/10.1130/B30154.1.

Quigley, M.C., Yu, L.J., Gregory, C., Corvino, A., Sandiford, M., Wilson, C.J.L., Liu, X.H., 2008. U–Pb SHRIMP zircon geochronology and T–t–d history of the Kampa Dome, southern Tibet. Tectonophysics 446, 97–113.

Spring, L., Bussy, F., Vannay, J.C., Hunon, S., Cosca, M.A., 1993. Early Permian granitic dikes of alkaline affinity in the Indian High Himalaya of upper Lahul and SE Zanskar: geochemical characterization and geotectonic implications. In: Treloar, P.J., Searle, M. (Eds.), Himalayan tectonics. Geological Society Special Publications, Geological Society of London, London, United Kingdom, pp. 251–264.

Tapponnier, P., Xu, Z.Q., Françoise, R., Bertrand, M., Nicolas, A., Gérard, W., Yang, J.S., 2001. Oblique stepwise rise and growth of the Tibet Plateau. Science 294 (5547), 1671–1677. http://dx.doi.org/10.1126/science.105978.

van Hinsbergen, D.J.J., Lippert, P.C., Dupont-Nivet, G., McQuarrie, N., Doubrovine, P.V., Spakman, W., Torsvik, T.H., 2012. Greater India Basin hypothesis and a two-stage Cenozoic collision between India and Asia. Proceedings of the National Academy of Sciences 109 (20), 7659–7664.

Van Wyck, N., Williams, I.S., 2002. Age and provenance of basement metasediments from the Kubor and Bena Bena Terranes, central Highlands, Papua New Guinea: constraints on the tectonic evolution of the northern Australian cratonic margin. Australian Journal of Earth Sciences 49 (3), 565–577.

Wen, D.R., Liu, D.Y., Chung, S.L., Chu, M.F., Ji, J.Q., Zhang, Q., Song, B., Lee, T.Y., Yeh, M.W., Lo, C.H., 2008. Zircon SHRIMP U–Pb ages of the Gangdese batholith and implications for Neotethyan subduction in southern Tibet. Chemical Geology 252 (3–4), 191–201.

Woodhead, J., Hergt, J., Shelley, M., Eggins, S., Kemp, R., 2004. Zircon Hf-isotope analysis with an excimer laser, depth profiling, ablation of complex geometries, and concomitant age estimation. Chemical Geology 209, 121–135. http://dx.doi.org/10.1016/j.chemgeo.2004.026.

Woodhead, J.D., Hellstrom, J., Hergt, J., Greig, A., Maas, R., 2007. Isotopic and elemental imaging of geological materials by laser ablation inductively coupled plasma-mass spectrometry. Geostandards and Geoanalytical Research 31 (4), 331–343.

Wu, F.Y., Ji, W.Q., Liu, C.Z., Chung, S.L., 2010. Detrital zircon U–Pb and Hf isotopic data from the Xigaze fore-arc basin: constraints on Transhimalayan magmatic evolution in southern Tibet. Chemical Geology 271, 13–25.

Yang, J.S., Xu, Z.Q., Li, Z.L., Xu, X.Z., Li, T.F., Ren, Y.F., Li, H.Q., Chen, S.Y., Robinson, P.T., 2009. Discovery of an eclogite belt in the Lhasa terrane, Tibet: a new border for Palaeo-Tethys? Journal of Asian Earth Sciences 34, 76–89.

Yin, A., 2006. Cenozoic evolution of the Himalayan orogen as constrained by alongstrike variations of structural geometry, exhumation history, and foreland sedimentation. Earth-Science Reviews 76, 1–134.

Yin, A., Harrison, T.M., 2000. Geologic evolution of the Himalayan–Tibetan orogen. Annual Review of Earth and Planetary Sciences 28, 211–280.

Yin, J.X., Xu, J.T., Liu, C.J., Li, H., 1988. The Tibetan plateau: regional stratigraphic context and previous work. Philosophical Transactions of the Royal Society of London (A) 327, 5–52.

Zeng, L.S., Liu, J., Gao, L., Chen, F.Y., Xie, K.J., 2009. Early Mesozoic high-pressure metamorphism within the Lhasa terrane, Tibet and implications for regional tectonics. Earth Science Frontiers 16 (2), 140–151.

Please cite this article as: Li, G., et al., Provenance of Late Triassic sediments in central Lhasa terrane, Tibet and its implication, Gondwana Research (2013), http://dx.doi.org/10.1016/j.gr.2013.06.019

Zeng, Q.G., Li, X.H., Xia, B., Xu, W.L., Nima, C., Pu, Q., Li, J., 2009. Heavy mineral assemblage and provenance analysis of the Upper Triassic in Renbu area, southern Tibet, China. Geological Bulletin of China 28 (1), 38–44 (Chinese with English abstract).

Zhai, Q.G., Li, C., Huang, X.P., 2007. The fragment of Palaeo-Tethys ophiolite from central Qiangtang, Tibet: geochemical evidence of metabasites in Guoganjianian. Science in China Series D: Earth Sciences 50, 1302–1309.

Zhai, Q.G., Wang, J., Li, C., Su, L., 2010. SHRIMP U–Pb dating and Hf isotopic analyses of Middle Ordovician meta-cumulate gabbro in central Qiangtang, northern Tibetan Plateau. Science China Earth Sciences 53, 657–664.

Zhang, H.F., Xu, C.W., Guo, J.Q., Zong, K.Q., Cai, H.M., Yuan, H.L., 2007. Indosinian orogenesis of the Gangdise terrane: evidences from zircon dating and petrogenesis of granitoids. Earth Science — Journal of China University of Geosciences 32 (2), 155–166 (Chinese with English abstract).

Zhao, W.J., Nelson, K.D., 1993. Project INDEPTH Team. Deep seismic reflection evidence for continental underthrusting beneath southern Tibet. Nature 366, 557–559.

Zheng, L.L., Geng, Q.R., Dong, H., Ou, C.S., Wang, X.W., 2003. The discovery and significance of the relic of ophiolitic mdlanges along the Yarlung Zangbo in the Bomi region, eastern Xizang. Sedimentary Geology and Tethyan Geology 23 (1), 27–30 (Chinese with English abstract).

Zhu, D.C., Pan, G.T., Chun, S.L., Liao, Z.L., Wang, L.Q., Li, G.M., 2008. SHRIMP zircon age and geochemical constraints on the origin of Early Jurassic volcanic rocks from the Yeba Formation, southern Gangdese in south Tibet. International Geology Review 50, 442–471.

Zhu, D.C., Mo, X.X., Niu, Y.L., Zhao, Z.D., Wang, L.Q., Pan, G.T., Wu, F.Y., 2009. Zircon U–Pb dating and in-situ Hf isotopic analysis of Permian peraluminous granite in the Lhasa terrane, southern Tibet: implications for Permian collisional orogeny and palaeogeography. Tectonophysics 469 (1–4), 48–60.

Zhu, D.C., Mo, X.X., Zhao, Z.D., Niu, Y.L., Wang, L.Q., Chu, Q., Pan, G.T., Xu, J.F., Zhou, C.Y., 2010. Presence of Permian extension-and arc-type magmatism in southern Tibet: palaeogeographic implications. Geological Society of America Bulletin 122 (7–8), 979–993.

Zhu, D.C., Zhao, Z.D., Niu, Y.L., Dilek, Y., Wang, L.Q., Mo, X.X., 2011. Lhasa terrane in southern Tibet came from Australia. Geology 39, 727–730.

Zhu, D.C., Zhao, Z.D., Niu, Y.L., Dilek, Y., Hou, Z.Q., Mo, X.X., 2013. The origin and pre-Cenozoic evolution of the Tibetan Plateau. Gondwana Research 23, 1429–1454.

Please cite this article as: Li, G., et al., Provenance of Late Triassic sediments in central Lhasa terrane, Tibet and its implication, Gondwana Research (2013), http://dx.doi.org/10.1016/j.gr.2013.06.019